

# An ESIPT-Based Ratiometric Fluorescent Probe for Highly Sensitive and Rapid Detection of Sulfite in Living Cells

Yupeng Liu,<sup>[a]</sup> Tian-Bing Ren,<sup>[a]</sup> Dan Cheng,<sup>[a]</sup> Jianing Hou,<sup>[a]</sup> Dongdong Su,<sup>\*,[b]</sup> and Lin Yuan<sup>\*,[a]</sup>

The novel ratiometric fluorescent probe HPQRB with an ESIPT effect based on Michael addition for highly sensitive and fast detection of sulfite in living HepG2 cells is reported. HPQRB can be easily synthesized by a two-step condensation reaction. HPQRB has a large emission shift ( $\Delta\lambda = 116$  nm), which is beneficial for fluorescence imaging research, and its sulfite-responsive site is based on a rhodamine-like structure with the emission peak at 566 nm, which decreases with increasing

sulfite concentration. and its HPQ structure always has an ESIPT effect throughout the reaction process, keeping the emission peak at 450 nm as a self-reference. In particular, HPQRB has high selectivity for sulfite and responds quickly (within 30 s) with a low detection limit (44 nM). Furthermore, HPQRB has been successfully used for fluorescence imaging of sulfite in HepG2 cells, demonstrating the superior ability to detect sulfite under physiological conditions.

## 1. Introduction

Sulfur dioxide ( $\text{SO}_2$ ) is widely used in the food industry as a food preservative, sanitizer for food containers and fermentation equipment and as moisture control agent, flavor modifier and puffing agent.<sup>[1]</sup> For example, it plays a crucial role in the production of wine.<sup>[2]</sup> At the same time, sulfur dioxide in the atmosphere, which is considered as a serious air pollutant, comes mainly from activities such as coal and oil burning in power plants or copper smelting. It is very soluble in water and to form sulfites or bisulfites that can enter the organisms with the food chain and are enriched and metabolized, eventually maintaining a range of normal concentrations.

In addition to food and atmospheric sources,  $\text{SO}_2$  can also be produced endogenously. In biosystems, gaseous  $\text{SO}_2$  usually presents in its hydrates ( $\text{SO}_3^{2-}$  and  $\text{HSO}_3^-$ ), and the toxicity of  $\text{SO}_2$  is mainly caused by its hydrates.<sup>[3–4]</sup> Many studies have shown that  $\text{SO}_2$  and its derivatives can participate in the regulation of vascular smooth muscle tension, lowering blood pressure<sup>[5–7]</sup> and other physiological processes,<sup>[8–9]</sup> but long-term exposure to sulfur dioxide derivatives in the environment can irritate the respiratory tract and nervous system.<sup>[10–11]</sup> At the same time, the deviation of sulfite concentration in the

organism from normal levels may indicate some pathological changes in the body. For example, serum sulfites in patients with acute pneumonia and cardiovascular diseases are significantly elevated.<sup>[12]</sup> Therefore, it is of vital importance to monitor the concentration of sulfite in the organisms.

Commonly used methods for detecting sulfite concentrations include high-performance liquid chromatography (HPLC),<sup>[13]</sup> electrochemical analysis,<sup>[14–15]</sup> capillary electrophoresis,<sup>[16]</sup> spectro-photometry<sup>[17]</sup> and flow injection analysis,<sup>[18]</sup> however, due to the cumbersome sample pretreatment and expensive instruments required, these methods are not suitable for routine analysis.<sup>[19]</sup> In contrast, fluorescent probes have been widely studied because of their simple operation, low damage to organisms, sensitive detection, high temporal and spatial resolution.<sup>[1,21–23]</sup> A series of probes for the detection of sulfite have been developed in recent years, in which ratiometric fluorescence sensing has received extensive attention as a detection tool with the potential for accurate and quantitative analysis.<sup>[24]</sup> Their advantages include high sensitivity and stability, independent of optical source intensity and instrument sensitivity.<sup>[25]</sup> Most of the reported fluorescent probes are based on aldehyde-based nucleophilic addition<sup>[26–27]</sup> or selective deprotection of acetylacetone.<sup>[28–29]</sup> However, some of them may be reactive to some sulfur-containing amino acids in the organism,<sup>[30]</sup> and most of them have high detection limits for sulfite and their sensitivity is not high enough.<sup>[31–32]</sup> Besides, some fluorescent probes have long response time and do not meet the sensitivity required for detection.<sup>[33–34]</sup> All of these factors limit their usefulness. Therefore, it is imperative to develop a probe that responds quickly to sulfite and with a low detection limit.

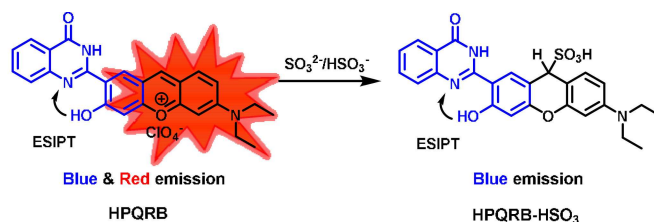
Herein, we report a ratiometric fluorescent probe **HPQRB** (Scheme 1) based on the Michael addition with ESIPT effect. **HPQRB** is capable of detecting sulfite with high selectivity in the presence of inorganic ions and biologically active small molecules typically found in the environment and in vivo. In particular, **HPQRB** has a low detection limit (44 nM) and achieves rapid response to sulfite within 30 seconds. It is worth

[a] Y. Liu, Dr. T.-B. Ren, Dr. D. Cheng, J. Hou, Prof. L. Yuan  
State Key Lab of Chemo/Biosensing and Chemometrics, College of Chemistry and Chemical Engineering, Hunan University  
Changsha 410082, P. R. China  
E-mail: lyuan@hnu.edu.cn

[b] Prof. D. Su  
Department of Chemistry and Chemical Engineering, Beijing University of Technology  
Beijing, 100124, P. R. China  
E-mail: chmsudd@bjut.edu.cn

Supporting information for this article is available on the WWW under <https://doi.org/10.1002/open.201900242>

© 2019 The Authors. Published by Wiley-VCH Verlag GmbH & Co. KGaA. This is an open access article under the terms of the Creative Commons Attribution Non-Commercial NoDerivs License, which permits use and distribution in any medium, provided the original work is properly cited, the use is non-commercial and no modifications or adaptations are made.



Scheme 1. Structure of probe HPQRB and its reaction mechanism with  $\text{SO}_3^{2-}$ .

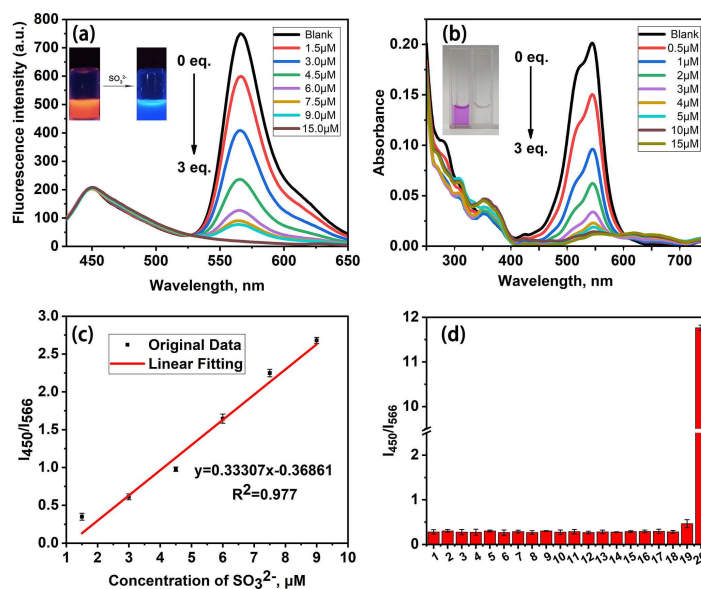


Figure 1. (a) Ratiometric fluorescence titration spectra of HPQRB (5  $\mu\text{M}$ ) upon addition of  $\text{SO}_3^{2-}$  (0–15  $\mu\text{M}$ ) in DMSO/PBS buffer (1/9, v:v, pH=7.4) at room temperature, Excitation at 388 nm. The inset photo shows the fluorescence colour changes of HPQRB with absence (left) and presence (right) of  $\text{SO}_3^{2-}$ . (b) UV/Vis titration spectra of HPQRB (5  $\mu\text{M}$ ) upon addition of  $\text{SO}_3^{2-}$  (0–15  $\mu\text{M}$ ) in DMSO/PBS buffer (1/9, v:v, pH=7.4) at room temperature. The inset photo shows the visible colour changes of HPQRB with absence (left) and presence (right) of  $\text{SO}_3^{2-}$ . (c) Linear relationship between the ratio of fluorescence intensity ( $I_{450}/I_{566}$ ) and the concentrations of  $\text{SO}_3^{2-}$ . (d) Selectivity responses of HPQRB (5  $\mu\text{M}$ ) to various relevant species in an aqueous solution (DMSO/PBS buffer = 1/9, v:v, pH=7.4) at room temperature. 1. Blank, 2.  $\text{Na}^+\text{Cl}^-$  (100  $\mu\text{M}$ ), 3.  $\text{Br}^-$  (100  $\mu\text{M}$ ), 4.  $\text{I}^-$  (100  $\mu\text{M}$ ), 5.  $\text{CO}_3^{2-}$  (100  $\mu\text{M}$ ), 6.  $\text{C}_2\text{O}_4^{2-}$  (100  $\mu\text{M}$ ), 7.  $\text{HPO}_4^{2-}$  (100  $\mu\text{M}$ ), 8.  $\text{K}^+\text{O}_2^{*-}$  (100  $\mu\text{M}$ ), 9.  $\text{Fe}^{2+}\text{SO}_4^{2-}$  (100  $\mu\text{M}$ ), 10.  $\text{NO}_3^-$  (100  $\mu\text{M}$ ), 11.  $\text{NO}_2^-$  (100  $\mu\text{M}$ ), 12.  $\text{H}_2\text{O}_2$  (100  $\mu\text{M}$ ), 13.  $\text{SCN}^-$  (100  $\mu\text{M}$ ), 14.  $\text{HOCl}$  (100  $\mu\text{M}$ ), 15.  $\text{HCO}_3^-$  (100  $\mu\text{M}$ ), 16. Cys (100  $\mu\text{M}$ ), 17. Hcy (100  $\mu\text{M}$ ), 18. GSH (1 mM), 19.  $\text{H}_2\text{S}_2$  (100  $\mu\text{M}$ ), 20.  $\text{SO}_3^{2-}$  (15  $\mu\text{M}$ ).

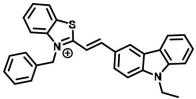
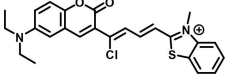
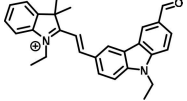
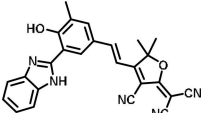
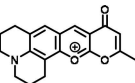
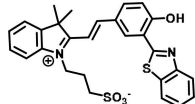
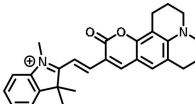
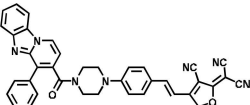
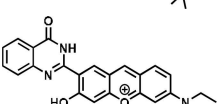
mentioning that HPQRB has two emission peaks with a large emission shift ( $\Delta\lambda = 116$  nm), wherein the fluorescence intensity of the emission peak at 450 nm remains unchanged before and after the entire reaction. In this case, we can use it as a self-reference to further improve the high sensitivity and inherent stability of the ratiometric fluorescent probe by self-calibration provided by monitoring two emissions.

## 2. Results and Discussion

To gain insight into the reaction between probe HPQRB and sulfite, fluorescence titration and UV/Vis absorption titration were performed respectively (Figure 1). In the fluorescence titration experiment, we found that it is a ratiometric fluorescent probe with two emission peaks at 450 nm and 566 nm, respectively. The emission shift is as high as 116 nm ( $\Delta\lambda = 116$  nm), which is beneficial for fluorescence imaging studies. As the sulfite concentration increased, the fluorescence intensity of the sample solution at 566 nm gradually decreased,

while the fluorescence intensity at 450 nm remained almost unchanged. Finally, when the sulfite concentration is 3 equivalents of the probe concentration, the fluorescence at 566 nm is minimized and hardly changes (Figure 1a). The decrease in fluorescence intensity at 566 nm is due to the destruction of the conjugated structure caused by the Michael addition reaction between the rhodamine-like structure of probe HPQRB and sulfite. The HPQ structure in the probe always has an ESIPT effect throughout the reaction, that is why the fluorescence at 450 nm remains constant (Figure S3). The ratio of fluorescence intensity ( $I_{450}/I_{566}$ ) showed a good linear relationship with the concentration of sulfite, and the detection limit was calculated to be 44 nM (Figure 1c). Furthermore, the absorbance intensity of HPQRB at 550 nm gradually decreased in the presence of  $\text{SO}_3^{2-}$ , meanwhile the colour changed from pink to colourless (Figure 1b). The above results and discussion indicate that probe HPQRB can be used for the quantitative detection of sulfite.

To study the selectivity, HPQRB (5  $\mu\text{M}$ ) was then treated with various biological species. As shown in Figure 1d, probe

Ratiometric fluorescent probes	Excitation/nm	Emission/nm (Before & After)	Emission shift/nm	LOD	Response time	References
	345	600/483	117	161 nM	35 s	[35]
	460	749/490	259	1220 nM	5 min	[36]
	–	570/445	125	1290 nM	1.5 min	[37]
	400	664/482	152	82 nM	8 min	[38]
	490	590/537	53	440 nM	7 min	[39]
	390	590/450	140	340 nM	15 min	[40]
	470	680/515	165	530 nM	6 min	[41]
	380	640/465	175	62 nM	2 min	[42]
	388	566/450	116	44 nM	30 s	This work

HPQRB (5  $\mu\text{M}$ ) was not only inert to those common anion and cation, such as  $\text{Cl}^-$ ,  $\text{Br}^-$ ,  $\text{I}^-$ ,  $\text{CO}_3^{2-}$ ,  $\text{C}_2\text{O}_4^{2-}$ ,  $\text{HPO}_4^{2-}$ ,  $\text{SO}_4^{2-}$ ,  $\text{NO}_3^-$ ,  $\text{NO}_2^-$ ,  $\text{SCN}^-$ ,  $\text{HCO}_3^-$ ,  $\text{Na}^+$ ,  $\text{K}^+$ ,  $\text{Fe}^{2+}$  (100  $\mu\text{M}$  for each), but also had negligible ratiometric signals to the reactive sulfur species (GSH (1 mM), Cys,  $\text{H}_2\text{S}_2$  and Hcy (others for 100  $\mu\text{M}$ ) and reactive oxygen ( $\text{O}_2^{\cdot-}$ ,  $\text{H}_2\text{O}_2$ , HClO) (100  $\mu\text{M}$  for each). However, just with 15  $\mu\text{M}$   $\text{SO}_3^{2-}$  added, a significant increase in fluorescence ratio at 450 nm and 566 nm ( $I_{450}/I_{566}$ ) was observed. We also carried out a competitive selectivity responses of HPQRB (5  $\mu\text{M}$ ) to  $\text{SO}_3^{2-}$  (15  $\mu\text{M}$ ) when coexisting with other biological species in an aqueous solution (DMSO/PBS buffer = 1/9, v:v, pH = 7.4) at room temperature (Figure S2). These results indicated the superior selectivity of HPQRB for  $\text{SO}_3^{2-}$  over other relevant species (Table 1).

To investigate the response time of the probe to sulfite, we added probe HPQRB (5  $\mu\text{M}$ ) to the solution and performed a fluorescence intensity time scan of 566 nm without the addition of sulfite, and started timing at the same time. When the scan was carried out for 120 seconds, sulfite (15  $\mu\text{M}$ ) was quickly added and time scanning was continued until the fluorescence

intensity no longer decreased. After processing and analyzing the experimental data, we were surprised to find that the response of HPQRB (5  $\mu\text{M}$ ) to sulfite was completed within 30 seconds (Figure 2a). It can be seen that the probe can achieve a rapid response to sulfite, which is superior to some of the currently reported fluorescent probes (Table 1). To further

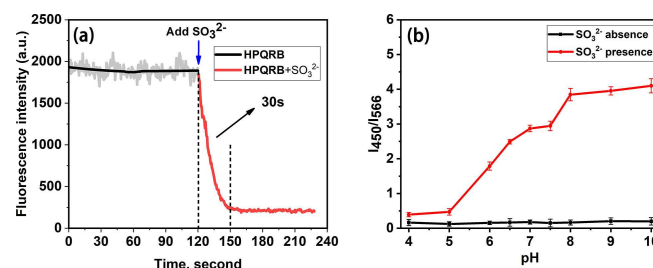


**Figure 2.** (a) Time scan of the fluorescence intensity of the blank probe (5  $\mu\text{M}$ ) sample before and after the addition of sulfite (15  $\mu\text{M}$ ). (b) The plot of the ratio of fluorescence intensity ( $I_{450}/I_{566}$ ) in DMSO/PBS buffer (1/9, v:v) and different pH.

investigate the effect of ambient pH on the detection of sulfite performance by probe HPQRB, we established two control experiments in different pH ranges (pH=4–10): a group of added sulfite and the other group without sulfite. We found that the ratio of fluorescence intensity ( $I_{450}/I_{566}$ ) of the group without sulfite was hardly changed with pH. As shown in Figure 2b, the probe HPQRB has high stability at different pH conditions. When the environment is very acidic, the addition reaction is blocked. As shown in pH=4–5, the fluorescence intensity at 566 nm was not completely reduced, indicating that high concentrations of hydrogen ions inhibited the addition of probe HPQRB and sulfite. When the environment is too alkaline (pH=8–10), the hydroxide ions undergo an addition reaction with the probe HPQRB, which enhances the fluorescence at 450 nm. Even so, we can still see from Figure 2b that probe HPQRB has good sulfite detection at pH=6–8 close to the physiological environment (pH=7.4). These results illustrate the potential of probe HPQRB to detect sulfite under physiological conditions.

At the beginning of the probe HPQRB design, we plan to link the reported HPQ<sup>[43]</sup> and rhodamine-like structure together. Thus, HPQRB retains the ESIPT effect of HPQ in solution to emit blue fluorescence as self-referencing, while the other end of the rhodamine-like structure emits orange-red fluorescence. When the probe HPQRB and sulfite undergo the 1, 4-Michael addition reaction to form the product HPQRB-HSO<sub>3</sub>, the orange-red fluorescence is reduced (Scheme 1). We tried to purify HPQRB-HSO<sub>3</sub>, but it did not succeed. Finally, we decided to use ESI-MS to study the reaction mechanism. We added a small amount of sulfite to the stock solution and then performed mass spectra. When in positive ion mode (M<sup>+</sup>), there is only the peak of 412 (m/z) for HPQRB, while when in negative ion mode (M<sup>-</sup>), there is only the peak of 492 (m/z) for HPQRB-HSO<sub>3</sub>. The results shown in Figure 3 confirm our design process.

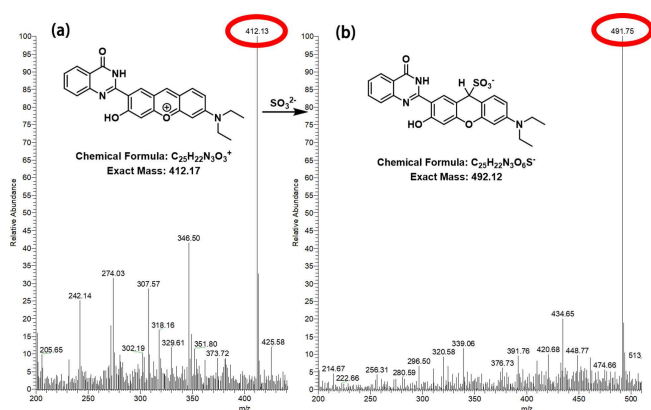


**Figure 3.** (a) ESI-MS of HPQRB m/z 412.13 (M<sup>+</sup>). (b) ESI-MS of HPQRB-HSO<sub>3</sub> m/z 491.75 (M<sup>-</sup>).

Encouraged by the superior performance of probe HPQRB in the above studies, we further explored its bioimaging capabilities in living cells. First, we performed cytotoxicity assays on HepG2 cells. According to the MTT test results, the HepG2

cell viability remained above 85% (Figure S1) after treatment with probe HPQRB (0–10.0 μM) for 12 hours, indicating low cytotoxicity of probe HPQRB.

We next incubated HepG2 cells with probe HPQRB (5 μM) for 1 hour, then continued to incubate for half an hour with the addition of different concentrations of sulfite (0–20 μM), and then performed fluorescence imaging. The fluorescent image is recorded under two channels, the blue channel and red channel. As shown in Figure 4, as the sulfite concentration increases, the fluorescence intensity of the blue channel remains almost constant, while the red channel reduced significantly. These results are in line with our expectations, indicating that the probe is capable of detecting different concentrations of sulfite in living cells.

Due to the complexity of the intracellular physiological environment, we decided to further explore the inhibitory effect of HCHO on the detection of sulfite by HPQRB.<sup>42</sup> Three groups of HepG2 cells were incubated in the medium containing probe HPQRB for 30 minutes. The first group was used as control, the second group and the third group were separately added with sulfite (20 μM) and formaldehyde (50 μM), and the incubation was continued for half an hour, followed by a third group of sulfites (20 μM) added for another half hour incubation before fluorescent image. The ratio image shows that formaldehyde has a significant inhibitory effect on sulfite detection by HPQRB.

### 3. Conclusions

In summary, we have developed a new type of Michael-based ratiometric fluorescent probe for the detection of sulfite, and because the probe HPQRB has an ESIPT effect, the fluorescence intensity at 450 nm can be used as a self-reference in the detection of sulfite to eliminate the interference of environmental factors. The probe HPQRB is a sensitive, efficient and rapidly responsive tool for the detection of sulfite, and the color of the solution changes from red to colourless for easy visual observation with great commercial potential, such as for the production of test strips for sulfite detection. At the same time, preliminary cell experiments show that probe HPQRB has low cytotoxicity and can detect intracellular sulfite well, which has great potential for living cell detection and imaging research.

## Experimental Section

### General

Because of the dissociation equilibrium between sulfite and bisulfite, they are present in aqueous solution at the same time, so in this article, sulfite is used instead of the above two substances.

### Determination of the Detection Limit

The detection limit was calculated based on fluorescence titration. In the fluorescence titration experiment, the fluorescence intensity ratio of HPQRB at 450 nm and 566 nm ( $I_{450}/I_{566}$ ) varies linearly with

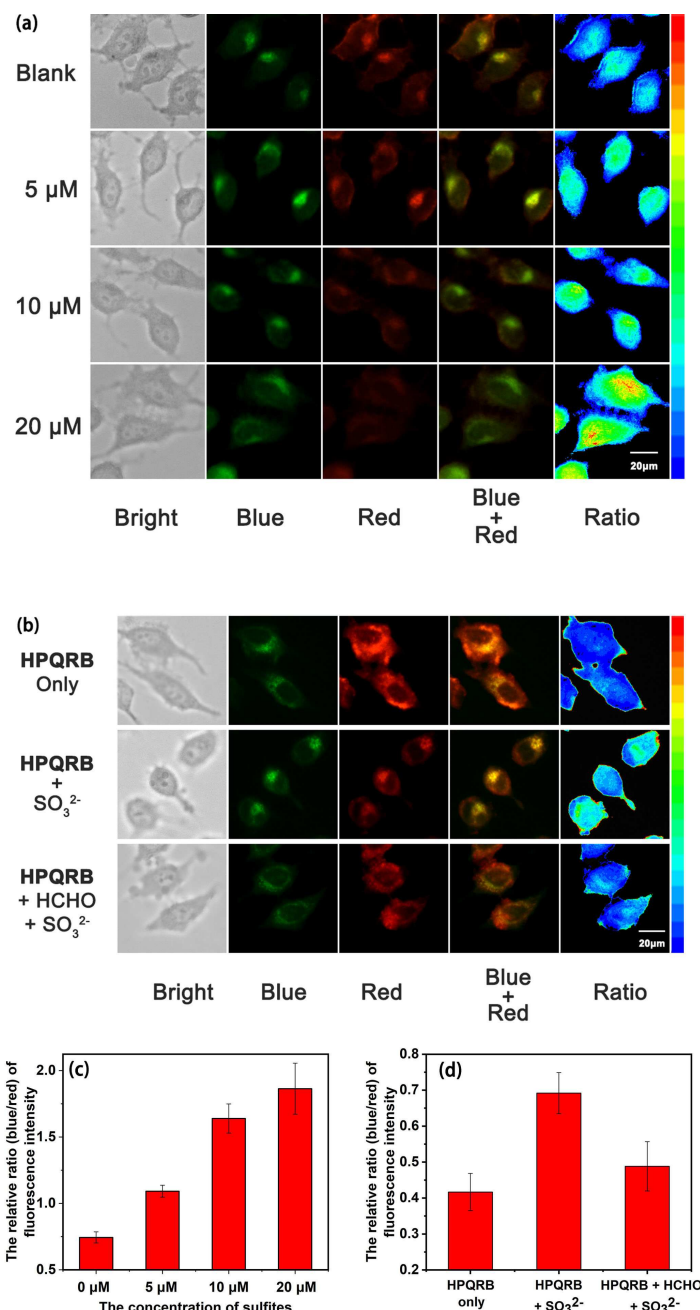


**Figure 4.** (a) Fluorescence imaging of HepG2 cells which were incubated for one hour in the presence of probe HPQRB (5 μM), 5 μM, 10 μM, and 20 μM sulfite for half an hour for fluorescence imaging. Images of the bright channel, the blue channel, and the red channel are acquired separately. (b) Fluorescence imaging of HPQRB in HepG2 cells with inhibitory effect of HCHO on detection of sulfite. (c) Histogram of the relative ratio of fluorescence intensity (blue/red). (d) Histogram of HPQRB in HepG2 cells with inhibitory effect of HCHO on detection of sulfite. Green fluorescence was collected under blue channel while the red fluorescence was collected under red channel.

the sulfite concentration. The detection limit was calculated based on the formula<sup>[44]</sup> as followed:

$$\text{Detection Limit} = 3\sigma/k$$

Where  $\sigma$  is the standard deviation of the blank solution and  $k$  is the slope of the calibration curve. The values of  $\sigma$  and  $k$  used to calculate the detection limit are 0.0049 and  $3.33 \times 10^5 \text{ M}^{-1}$ , respectively.

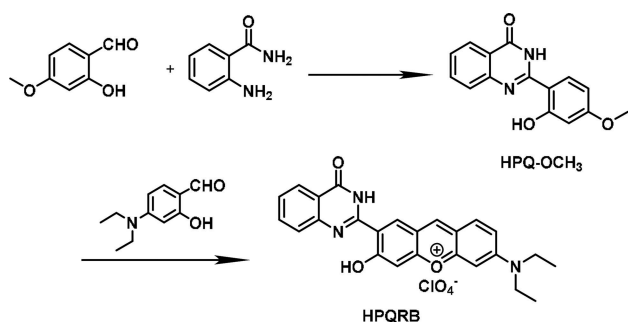
### Synthetic Procedures and Methods

**Synthesis of HPQ-OCH<sub>3</sub>.** Added 2-aminobenzamide (340 mg, 2.5 mmol) to a solution of ethanol (40 mL) containing 2-hydroxy-4-methoxybenzaldehyde (380 mg, 2.5 mmol), and the solution was stirred in an ice bath for 10 minutes. It was then stirred in an oil bath at 80 °C for 30 minutes. After the addition of the catalyst TsOH (20 mg), the reaction was continued for another 60 minutes. When the mixture was cooled to room temperature, DDQ (560 mg, 2.5 mmol) was added and stirred overnight. HPQ-OCH<sub>3</sub> was filtered



and dried as a light brown solid (509 mg) with the yield of 76%.  $^1\text{H}$  NMR (400 MHz, DMSO- $d_6$ )  $\delta$  14.38 (s, 1H), 12.39 (s, 1H), 8.20 (d,  $J=8.8$  Hz, 1H), 8.13 (d,  $J=7.8$  Hz, 1H), 7.83 (t,  $J=7.5$  Hz, 1H), 7.71 (d,  $J=8.1$  Hz, 1H), 7.51 (t,  $J=7.3$  Hz, 1H), 6.55 (d,  $J=12.8$  Hz, 2H), 3.82 (s, 3H).  $^{13}\text{C}$  NMR (100 MHz, DMSO- $d_6$ )  $\delta$  164.2, 163.3, 162.0, 154.4, 146.2, 135.5, 129.2, 126.9, 126.5, 125.8, 120.8, 107.0, 106.5, 102.2, 55.9. MS-ESI:  $m/z$ ,  $\text{C}_{15}\text{H}_{13}\text{N}_2\text{O}_3^+$  ( $\text{M}+\text{H}^+$ ), calculated: 269.1, found 269.1.

**Synthesis of HPQRB (Scheme 2).** HPQ-OCH<sub>3</sub> (108 mg, 4.0 mmol) and 4-(diethylamino)-2-hydroxybenzaldehyde (78 mg, 4.0 mmol) were added to the reactor, followed by the addition of 2 mL of methane-sulfonic acid, and then reacted in an oil bath at 90 °C for 4 hours. After cooling the reaction to room temperature, the reaction solution was poured into 100 mL ice water, and 2 mL of perchloric acid was added. After the solid precipitated, it was filtered off and dried. The product was purified by column chromatography ( $\text{CH}_2\text{Cl}_2/\text{EtOH}=80/1$ ) to afford HPQRB as a scarlet solid (121 mg) and the yield was 74%.  $^1\text{H}$  NMR (400 MHz,  $\text{CDCl}_3$ )  $\delta$  8.72 (s, 1H), 8.20 (s, 1H), 8.13 (d,  $J=8.0$  Hz, 1H), 7.71 (s, 1H), 7.67 (s, 1H), 7.51 (d,  $J=8.3$  Hz, 1H), 7.38 (s, 1H), 6.77 (d,  $J=8.8$  Hz, 1H), 6.53 (s, 1H), 6.49 (s, 1H), 3.45 (d,  $J=6.1$  Hz, 4H), 1.21 (s, 6H).  $^{13}\text{C}$  NMR (100 MHz,  $\text{CDCl}_3$ )  $\delta$  158.1, 156.9, 154.9, 144.8, 134.3, 133.8, 132.5, 130.5, 125.6, 125.5, 124.0, 120.4, 113.5, 112.3, 112.1, 105.4, 95.7, 45.1, 11.7. MS-ESI:  $m/z$ ,  $\text{C}_{25}\text{H}_{22}\text{N}_3\text{O}_3^+$  ( $\text{M}^+$ ), calculated: 412.2, found 412.2.



Scheme 2. The synthetic route of probe HPQRB.

### Reaction Mechanism Study

Analytes include different inorganic salts such as  $\text{K}_2\text{C}_2\text{O}_4$ ,  $\text{K}_2\text{O}$ ,  $\text{NaI}$ ,  $\text{NaNO}_3$ ,  $\text{NaOCl}$ ,  $\text{NaBr}$ ,  $\text{NaHCO}_3$ ,  $\text{NaSCN}$ ,  $\text{NaNO}_2$ ,  $\text{Na}_2\text{HPO}_4$ ,  $\text{Na}_2\text{SO}_4$ ,  $\text{Na}_2\text{CO}_3$ ,  $\text{NaCl}$ ,  $\text{Na}_2\text{S}_2$ ,  $\text{Na}_2\text{SO}_3$  and active small biological molecules like  $\text{H}_2\text{O}_2$ , homocysteine (Hcy), cysteine (Cys) and glutathione (GSH). The stock solutions of these analytes were all 10 mM and all were dissolved in deionized water except that  $\text{KO}_2$  was dissolved in DMSO. The probe HPQRB was dissolved in DMSO to afford the stock solution (0.5 mM). The concentration of the sample solution (PBS:DMSO=9:1,  $v/v$ , pH=7.4) used for the absorption and fluorescence determination test is 5.0  $\mu\text{M}$ , which is diluted by the stock solution.

### Acknowledgements

This work was supported by the National Natural Science Foundation of China (No. 21877029, 21735001) and the National

College Student Innovation and Entrepreneurship Training Program (201810532053).

### Conflict of Interest

The authors declare no conflict of interest.

**Keywords:** fluorescent probe · sulfite · ratiometric probes · fluorescence · imaging studies

- [1] W. Chen, Q. Fang, D. Yang, H. Zhang, X. Song, J. Foley, *Anal. Chem.* **2015**, *87*, 609–616.
- [2] B. Palenzuela, B. M. Simonet, A. Ríos, M. Valcárcel, *Anal. Chim. Acta* **2005**, *535*, 65–72.
- [3] X. Shi, *J. Inorg. Biochem.* **1994**, *56*, 155–165.
- [4] N. Sang, Y. Yun, G. Yao, H. Li, L. Guo, G. Li, *Toxicol. Sci.* **2011**, *124*, 400–413.
- [5] W. Xu, J. Li, W. Zhang, Z. Wang, J. Wu, X. Ge, J. Wu, Y. Cao, Y. Xie, D. Ying, Y. Wang, L. Wang, Z. Qiao, J. Jia, *Environ. Pollut.* **2018**, *242*, 90–97.
- [6] Z. Meng, Z. Yang, J. Li, Q. Zhang, *Chemosphere* **2012**, *89*, 579–584.
- [7] V. S. Lin, W. Chen, M. Xian, C. J. Chang, *Chem. Soc. Rev.* **2015**, *44*, 4596–4618.
- [8] W. Xu, C. L. Teoh, J. Peng, D. Su, L. Yuan, Y. Chang, *Biomaterials* **2015**, *56*, 1–9.
- [9] F. Cai, B. Hou, S. Zhang, H. Chen, S. Ji, X. Shen, H. Liang, *J. Mater. Chem. B*, **2019**, *7*, 2493–2498.
- [10] X. Zheng, H. Li, W. Feng, H. Xia, Q. Song, *ACS Omega* **2018**, *3*, 11831–11837.
- [11] N. Sang, Y. Yun, H. Li, L. Hou, M. Han, G. Li, *Toxicol. Sci.* **2010**, *114*, 226–236.
- [12] J. Sunyer, F. Ballester, A. L. Tertre, R. Atkinson, J. G. Ayres, F. Forastiere, B. Forsberg, J. M. Vonk, L. Bisanti, J. Medina, J. Schwartz, K. Katsouyanni, *Eur. Heart J.* **2003**, *24*, 752–760.
- [13] S. Theisen, R. Hansch, L. Kothe, U. Leist, R. Galensa, *Biosens. Bioelectron.* **2010**, *26*, 175–181.
- [14] Ü. T. Yilmaz, G. Somer, *Anal. Chim. Acta* **2007**, *603*, 30–35.
- [15] M. H. Pournaghi-Azar, M. Hydarpour, H. Dastangoo, *Anal. Chim. Acta* **2003**, *497*, 133–141.
- [16] A. N. de Macedo, M. I. Y. Jiwa, J. Macri, V. Belostotsky, S. Hill, P. Britz-McKibbin, *Anal. Chem.* **2013**, *85*, 11112–11120.
- [17] S. S. M. Hassan, M. S. A. Hamza, A. H. K. Mohamed, *Anal. Chim. Acta* **2006**, *570*, 232–239.
- [18] H. Mana, U. Spohn, *Anal. Chem.* **2001**, *73*, 3187–3192.
- [19] M. Wu, T. He, K. Li, M. Wu, Z. Huang, X. Yu, *Analyst* **2013**, *138*, 3018–3025.
- [20] D. Cheng, W. Xu, L. Yuan, X. Zhang, *Anal. Chem.* **2017**, *89*, 7693–7700.
- [21] T. Ren, W. Xu, W. Zhang, X. Zhang, Z. Wang, Z. Xiang, L. Yuan, X. Zhang, *J. Am. Chem. Soc.* **2018**, *140*, 7716–7722.
- [22] D. Cheng, J. Peng, Y. Lv, D. Su, D. Liu, M. Chen, L. Yuan, X. Zhang, *J. Am. Chem. Soc.* **2019**, *141*, 6352–6361.
- [23] T.-B. Ren, W. Xu, Q.-L. Zhang, X.-X. Zhang, S.-Y. Wen, H.-B. Yi, L. Yuan, X.-B. Zhang, *Angew. Chem. Int. Ed.* **2018**, *57*, 7473–7477; *Angew. Chem.* **2018**, *130*, 7595–7599.
- [24] C. Duan, J. Zhang, Y. Hu, L. Zeng, D. Su, G. Bao, *Dyes Pigments* **2019**, *162*, 459–465.
- [25] W. Lin, L. Long, L. Yuan, Z. Cao, B. Chen, W. Tan, *Org. Lett.* **2008**, *10*, 5577–5580.
- [26] C. Yu, M. Luo, F. Zeng, S. Wu, *Anal. Methods* **2012**, *4*, 2638–2640.
- [27] X. Cheng, H. Jia, J. Feng, J. Qin, Z. Li, *Sens. Actuators B* **2013**, *184*, 274–280.
- [28] X. Ma, C. Liu, Q. Shan, G. Wei, D. Wei, Y. Du, *Sens. Actuators B* **2013**, *188*, 1196–1200.
- [29] X. Gu, C. Liu, Y. Zhu, Y. Zhu, *J. Agric. Food Chem.* **2011**, *59*, 11935–11939.
- [30] M. H. Lee, J. S. Kim, J. L. Sessler, *Chem. Soc. Rev.* **2015**, *44*, 4185–4191.
- [31] G. Zhang, R. Ji, X. Kong, F. Ning, A. Liu, J. Cui, Y. Ge, *RSC Adv.* **2019**, *9*, 1147–1150.
- [32] Y. Yao, Q. Sun, Z. Chen, R. Huang, W. Zhang, J. Qian, *Talanta* **2018**, *189*, 429–436.
- [33] M. Wu, K. Li, C. Li, J. Hou, X. Yu, *Chem. Commun.* **2014**, *50*, 183–185.

- [34] Y. Zhang, L. Guan, H. Yu, Y. Yan, L. Du, Y. Liu, M. Sun, D. Huang, S. Wang, *Anal. Chem.* **2016**, *88*, 4426–4431.
- [35] H. Li, X. Zhou, J. Fan, S. Long, J. Du, J. Wang, X. Peng, *Sens. Actuators B* **2018**, *254*, 709–718.
- [36] X. Yang, Y. Yang, T. Zhou, M. Jin, X. Jing, C. Miao, W. Li, *J. Photochem. Photobiol. A* **2019**, *372*, 212–217.
- [37] K. Bi, R. Tan, R. Hao, L. Miao, Y. He, X. Wu, J. Zhang, X. Rui, *Chin. Chem. Lett.* **2019**, *30*, 545–548.
- [38] T. Niu, T. Yu, G. Yin, H. Chen, P. Yin, H. Li, *Analyst* **2019**, *144*, 1546.
- [39] J. Li, Y. Gao, H. Guo, X. Li, H. Tang, J. Li, Y. Guo, *Dyes Pigm.* **2019**, *163*, 285.
- [40] Y. Zhang, L. Guan, H. Yu, Y. Yan, L. Du, Y. Liu, M. Sun, D. Huang, S. Wang, *Anal. Chem.* **2016**, *88*, 4426–4431.
- [41] Y. Yao, Q. Sun, Z. Chen, R. Huang, W. Zhang, J. Qian, *Talanta* **2018**, *189*, 429–436.
- [42] G. Zhang, R. Ji, X. Kong, F. Ning, A. Liu, J. Cui, Y. Ge, *RSC Adv.* **2019**, *9*, 1147–1150.
- [43] L. Zhou, X. Zhang, Y. Lv, C. Yang, D. Lu, Y. Wu, Z. Chen, Q. Liu, W. Tan, *Anal. Chem.* **2015**, *87*, 5626–5631.
- [44] G. J. Mohr, *Chem. Commun.* **2002**, 2646–2647.

---

 Manuscript received: July 19, 2019

Revised manuscript received: August 19, 2019